

# Influence of fibre taper on the work of fibre pull-out in short fibre composite fracture

X. W. Ng · D. W. L. Hukins · K. L. Goh

Received: 22 July 2009 / Accepted: 18 November 2009 / Published online: 4 December 2009  
© Springer Science+Business Media, LLC 2009

**Abstract** A model has been formulated to determine the work of pull-out,  $U$ , of an elastic fibre as it shear-slides out of a plastic matrix in a fractured composite. The fibres considered in the analysis have the following shapes: uniform cylinder and ellipsoidal, paraboloidal or conical tapers. Energy transfer at the fibre–matrix interface is described by an energy density parameter which is defined as the ratio of  $U$  to the fibre surface area. The model predicts that the energy required to pull out a tapered fibre is small because the energy transfer at the fibre–matrix interface to overcome friction is small. In contrast, the pull-out energy of a uniform cylindrical fibre is large because the energy transfer is large. The pull-out energies of the paraboloidal and ellipsoidal fibres lay between those for the uniform cylindrical and the conical fibres. With the exception of the uniform cylindrical fibre which yields a constant energy density, tapered fibres yield expressions for the energy density which depend on the fibre axial ratio,  $q$ . In particular, the energy density increases as  $q$  increases but converges at large  $q$ . By defining the critical axial ratio,  $q_0$ , as the limit beyond which  $u$  is independent of the fibre slenderness, our model predicts the value of  $q_0$  to be about 10. These results are applied to explain the mechanisms regulating fibre composite fracture.

## Introduction

This paper is concerned with the energy required to pull out a short fibre, which need not be a uniform cylinder, during fracture of a fibre-reinforced composite material. The energy required to pull out a uniform cylindrical fibre [1–6], including the transfer of stress between the matrix and fibre [7], has been calculated previously. However, recent research has considered the reinforcement of composites by fibres which need not be uniform cylinders [8, 9]. This research has focussed on the mechanisms of stress transfer using analytical approaches to address the reinforcement of a plastic matrix with elastic fibres [10], finite element (FE) models of reinforcing a plastic matrix with elastic fibres [11, 12] and FE models of reinforcing an elastic matrix with elastic fibres [12, 13] and fracture of fibres [14]. Figure 1 shows the shapes of the fibres considered in this, and previous, papers which we describe as being a uniform cylinder or having conical, paraboloidal or ellipsoidal tapers [10].

The response of a short-fibre reinforced composite material, subjected to an increasing tensile force, occurs in several stages [12, 13]. The first stage is elastic stress transfer from the surrounding matrix to the fibre [15]. For an elastic fibre embedded in and bonded to an elastic matrix, shear-lag analysis predicts that shear of the matrix over the fibre generates an interfacial shear stress which places the fibre in tension [4]. The interfacial shear stress is lower for tapered fibres than for a uniform cylindrical fibre [12]. The axial tensile stress peaks at the centre of a uniform cylindrical fibre and decreases non-linearly to zero at the fibre end. At the other extreme, the axial stress in a fibre with conical ends is a minimum at the fibre centre and rises gradually to a maximum near the ends [12, 13]. Concentrating stresses near the fibre end makes good sense because, should a portion near the end break, the effectiveness of the bulk of

---

X. W. Ng  
School of Materials Science and Engineering, Nanyang  
Technological University, Singapore 637457, Singapore

D. W. L. Hukins  
School of Mechanical Engineering, University of Birmingham,  
Edgbaston, Birmingham B15 2TT, UK

K. L. Goh (✉)  
School of Engineering, Monash University, Bandar Sunway,  
46150 Selangor Darul Ehsan, Malaysia  
e-mail: goh.kheng.lim@eng.monash.edu.my

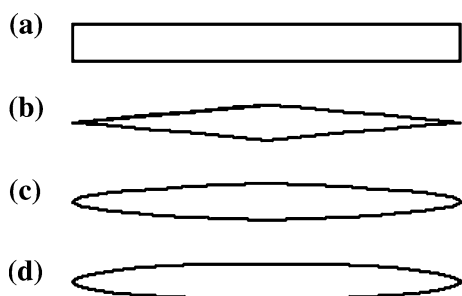


**Fig. 1** Shapes of the fibres considered in this paper: **a** cylindrical, **b** conical, **c** paraboloidal and **d** ellipsoidal

this fibre for reinforcement would not be appreciably compromised. However, concentrating stresses at the fibre centre means that the fibre length will be halved, if it breaks. It has been shown that stress distributions for the paraboloid and ellipsoid lay between those for the cylinder and the cone [12, 13].

In the second stage of failure, bond disruption occurs at the fibre–matrix interface and propagates as the applied force increases [16]. The matrix deforms plastically and flows over the fibre surface; shear-sliding analysis predicts that a constant interfacial shear stress is generated as the matrix yields and flows over the fibre [4]. This stress is opposed by the tensile stress generated in the fibre, so that the debonded fibre is capable of providing tensile reinforcement [4]. Then, the axial stress peaks at the centre of the uniform cylindrical fibre and decreases linearly to zero at the end; at the other extreme, the conical fibre yields a constant axial stress distribution [10]. Stress distributions for the paraboloid and ellipsoid lay between those for the cylinder and the cone [10]. Thus, taper yields a more uniformly distributed axial stress throughout the fibre as compared to that from a uniform cylindrical fibre [10].

Finally, the material begins to fail by a variety of mechanisms: debonding at the fibre–matrix interface, fibre fragmentation, matrix cracking and fibre pull-out [12, 13]. The order and importance of these events depend on the properties of the materials that make up the composite [4]. Here we are concerned with pull-out of a fibre, following matrix cracking.

**Methods**

**Definitions**

Consider a fibre of length  $2L$  embedded in a matrix as shown in Fig. 2a. When the matrix cracks around the fibre, either the short or the long fibre fragment could slide out. However, since more energy will be required to pull out the long fragment, it is the short fragment that will be pulled

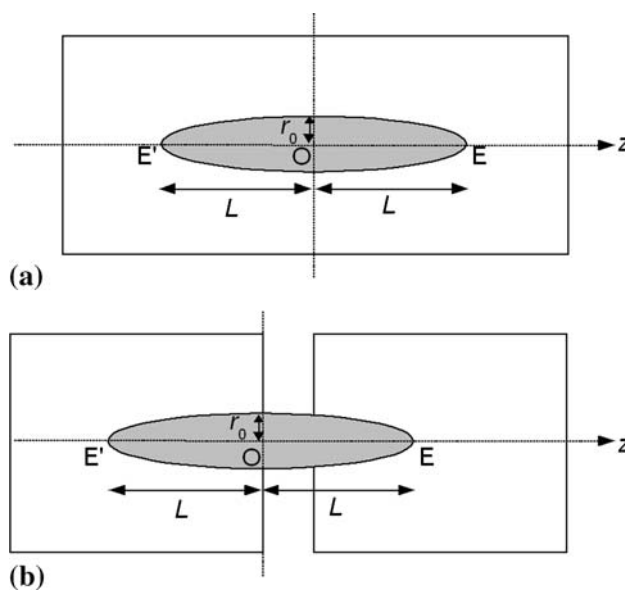


**Fig. 2** Models of **a** a fibre embedded in matrix and **b** fibre pull-out from the matrix. The model is axisymmetric about the axis so that only a plane about the axis is shown here. Also the centre of the fibre defines the origin, O, of the cylindrical polar coordinate system. The ends of the fibre are indicated by E and E'. The full model is obtained by rotating 180° about the z-axis to generate an axisymmetric fibre composite. Here,  $r_0$  represents the radius of the fibre, at the centre of the fibre, and  $L$  represents the half-length of the fibre

out. Therefore, the longest length of the fibre fragment to be pulled out is  $L$  and this length corresponds to the maximum pull-out energy.

In previous work [10], the origin, O, of the cylindrical polar coordinate system was defined to be at the fibre centre and the fibre-axis direction defined the  $z$ -axis. A fractional translation along the fibre, with respect to O, was defined by a fractional coordinate  $Z = z/L$  where  $-1 \leq Z \leq 1$  within a fibre. We will use this approach to describe fibre pull-out. During pullout, one matrix fracture surface is displaced from O, in the fibre-axis direction, as shown in Fig. 2b.

The radius,  $r$ , of a tapered fibre (Fig. 2) has its maximum value at O when  $r = r_0$ . The value of  $r$  then decreases to zero at the ends, E and E', of the fibre. The fibre axial ratio is defined as

$$q = L/r_0 \tag{1}$$

[10]. For a uniform cylindrical fibre,  $r$  is a constant; for the other fibre shapes it is a function of  $Z$ , as shown in Table 1 [10].

**Pull-out force**

A constant shear stress,  $\tau$ , acts at the fibre–matrix interface as the debonded fibre slides out of the matrix, during plastic stress transfer. This model is reasonable for

**Table 1** Expressions for the radius,  $r(Z)$ , axial stress  $\sigma_z(Z)$  and surface area of half a fibre,  $A$ , for the four fibre shapes shown in Fig. 1

Fibre shape	$R(Z)$	$\sigma_z(Z)$	$A$
Cylindrical	$L/q$	$-2\tau q[1 - Z]$	$2\pi r_0 L$
Conical	$\{L/q\}[1 - Z]$	$-\tau q$	$\pi r_0 \sqrt{r_0^2 + L^2}$
Paraboloidal	$\{L/q\}\sqrt{1 - Z}$	$-\frac{4\tau q}{3}\sqrt{1 - Z}$	$\frac{\pi r_0}{6L^2} \left[ \{r_0^2 + 4L^2\}^{3/2} - r_0^3 \right]$
Ellipsoidal	$\{L/q\}\sqrt{1 - Z^2}$	$-\tau q \left\{ \frac{\pi/2 - \sin^{-1} Z}{1 - Z^2} - \frac{Z}{\sqrt{1 - Z^2}} \right\}$	$\pi r_0^2 + \frac{\pi r_0 L^2}{\sqrt{L^2 - r_0^2}} \sin^{-1} \left( \frac{\sqrt{L^2 - r_0^2}}{L} \right)$

composite materials in which stiff fibres reinforce a weak matrix [10]. In this case, the molecular basis of a constant value for  $\tau$  corresponds to a constant number of macro-molecular interactions per unit area between the matrix and the fibre. Shear of the interface involves overcoming these intermolecular forces at the interface.

Axial stresses are generated because the force acting to pull out the fibre from the matrix generates an interfacial shear stress  $\tau$ . Consider the fibre end, E, at a distance  $Z$  from O (Fig. 2b). Let  $\sigma_z(Z)$  be the axial stress in the embedded fibre. Within the embedded section of the fibre, the form of  $\sigma_z(Z)$  can be determined by solving the first order differential equation,

$$d[\sigma_z r^2]/dZ + 2\tau q = 0 \tag{2}$$

[10]. Table 1 presents the results obtained, by solving Eq. 2, for the fibre shapes considered here. During pull-out, when the fibre end, E, is at a distance  $Z$  from O (Fig. 2), the force applied to the fibre at O is given by

$$F(Z) = \pi r(Z)^2 \sigma(Z). \tag{3}$$

Note that the magnitude of  $F$  depends on  $Z$ . Equation 3 can be used to calculate  $F(Z)$ , for each fibre shape, from the expressions for  $r(Z)$  and  $\sigma_z(Z)$  (Table 1). Note that immediately after the fibre is pulled out of the matrix ( $Z = 1$ ), the force becomes zero.

**Pull-out energy**

The maximum energy to pull a fibre out of the matrix,  $U$ , is given by the work done to pull a length  $L$  of fibre embedded in the matrix,

$$U = L \int_1^0 F(Z) dZ \tag{4}$$

The pull-out energies for the four fibre shapes shown in Fig. 1 are obtained by substituting the expression for  $F(Z)$ , from Eq. 3, into Eq. 4 and using the appropriate expressions for  $r(Z)$  and  $\sigma_z(Z)$ , from Table 1.

In addition, Eq. 4 allows us to quantify the energy transfer to overcome frictional forces at the fibre–matrix interface using an energy density parameter defined by

$$u = U/A \tag{5}$$

where  $A$  is the surface area of one half of a fibre. This area is given by

$$A = 2\pi \int_0^1 r(Z) dZ \tag{6}$$

The surface area,  $A$ , for each of the four shapes shown in Fig. 1 is obtained by substituting the appropriate expression for  $r(Z)$  from Table 1 into Eq. 6; the results are shown in Table 1. Note that we are only concerned with the surface of the fibre adjacent to the fibre axis; for the uniform cylindrical fibre the end faces of the fibre were not considered in the calculation of  $A$ .

**Results**

The work of pull-out can be expressed in the form:

$$U = \alpha \pi \tau r_0 L^2 \tag{7}$$

where  $\alpha$  is a numerical factor that depends on the shape of the fibre; values of  $\alpha$  are given in Table 2, for each of the four fibre shapes shown in Fig. 1. The other variables in Eq. 7 are defined in “Definitions”. According to Eq. 7 and Table 2, the pull-out energy depends on fibre shape. In particular, the energies to pull out a conical fibre, a paraboloidal fibre and an ellipsoidal fibre are about 33, 53 and 67%, respectively, that of the uniform cylindrical fibre.

This paragraph is concerned with the expression for the pull-out energy,  $U$ , for a uniform cylinder which is given by substituting the value for  $\alpha$  from Table 2 into Eq. 7.

**Table 2** The predicted values of the parameters  $\alpha$  and  $\beta$  associated with the work of fibre pull-out (Eq. 7) and the interaction energy density (Eq. 8), respectively

Fibre shape	$\alpha$	$\beta$
Cylindrical	1	$\frac{1}{2\pi}$
Conical	1/3	$\frac{1}{3\pi} \frac{q}{\sqrt{1+q^2}}$
Paraboloidal	8/15	$\frac{16}{5\pi} \frac{q^3}{\{1+4q^2\}^{3/2} - 1}$
Ellipsoidal	2/3	$\frac{2}{3\pi} q \left\{ 1 + \frac{q^2}{\sqrt{q^2 - 1}} \sin^{-1} \left( \frac{\sqrt{q^2 - 1}}{q} \right) \right\}^{-1}$

This result is the same as that published previously [3]. The published result was obtained by calculating  $U$  directly from the interfacial stress,  $\tau$ . Although this approach is simplest for a uniform cylindrical fibre, it is simpler to calculate  $U$  from  $\sigma_z(Z)$  for a tapered fibre. That the two approaches give the same result for a uniform cylinder provides confirmation of the approach adopted here.

The energy transfer at the fibre–matrix interface for the four fibre shapes can be expressed in the form:

$$u = \beta\tau L \tag{8}$$

where  $\beta$  is a numerical factor that depends on the shape of the fibre; values of  $\beta$  are given in Table 2, for each of the four fibre shapes shown in Fig. 1. For the uniform cylindrical fibre  $\beta$  is a constant; for the other shapes,  $\beta$  depends on  $q$ . Figure 3 shows plots of  $u/\tau L$  versus  $q$ , evaluated by substituting the appropriate value for  $\beta$  from Table 2 into Eq. 8, assigning a value for  $q$  in the range 1–3500. The upper limit of  $q$  was selected to cover the variety of fibres available in engineering materials [17] and in biological tissues [18]. It is observed that, apart from uniform cylindrical fibre which yields a constant  $u/\tau L$ , in tapered fibres  $u/\tau L$  increases non-linearly as  $q$  increases at small  $q$  values. Beyond  $q = 10$ ,  $u/\tau L$  converges to 0.106, 0.126 and 0.134, for the conical fibre, the paraboloidal fibre and the ellipsoidal fibre, respectively. We note that these magnitudes of  $u/\tau L$  are lower than that of the uniform cylindrical fibre. Note also that the convergent limit of  $u/\tau L$  in tapered fibres corresponds to the beginning of rapid increment in the surface area as shown in the plots of  $A$  versus  $q$  in Fig. 4. Here,  $A$  was evaluated at values of  $q$  in the range of 1–3500, by fixing the value of  $r_0$  at unit length in arbitrary units (a.u.) and calculating the corresponding  $L$  from Eq. 1. Note that the units used for area and length are immaterial as long as they are consistent.

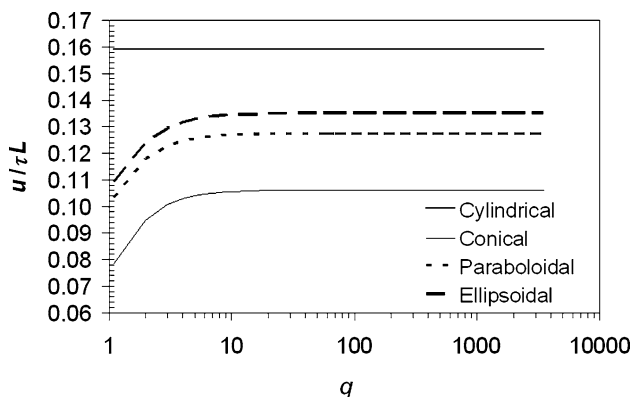


**Fig. 3** Graph of  $u/\tau L$  versus  $q$  for the following shapes: a cone, a paraboloid, an ellipsoid and a uniform cylinder

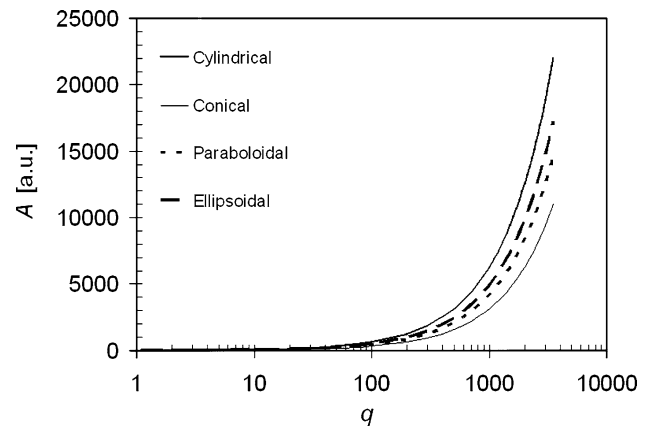


**Fig. 4** Graph of  $A$  versus  $q$  for the following shapes: a cone, a paraboloid, an ellipsoid and a uniform cylinder. Here,  $r_0$  and  $L$  were assigned lengths of the arbitrary units (a.u.) for determining  $A$ ; for further explanations see “Results”

### Discussion

Following from the discussion in “Introduction”, when the load applied to the fibre composite is sufficiently large, the composite fails. At this point, any fibres that were bonded to the matrix could fragment. Thereafter, two modes of failure could occur: (1) a circular crack propagating outwards into the matrix; (2) a cylindrical crack propagating along the fibre–matrix interface from the break point to the fibre end [19]. However, should the fibre not fragment, it could debond from the matrix if a crack wake (in the matrix) develops around the fibre [20]. Consequently, shear-sliding analysis predicts that a debonded fibre whose length is longer than the fibre critical length is most effectiveness for reinforcing the composite; the fibre take up stress and fragments when the stress level reaching magnitudes equal to the fracture stress of the fibre [4]. It follows that the critical length of the conical fibre is the longest; at the other extreme, the critical length of the uniform cylindrical fibre is the shortest. The critical lengths of intermediate fibre shapes, i.e. the paraboloidal fibre and the ellipsoidal fibre, lies between the two extremes of fibre shape [14]. Experiments have shown that the longer the fibres (assuming similar radii for all the fibres), the tougher, stronger and stiffer the composite [21].

Thus, the bulk of the load is supported by the matrix surrounding fibres whose length is shorter than the critical length because these fibres are ineffective for reinforcing the matrix [4]. If the matrix ruptures around the fibre; the fibre attempts to bridge the rupture site. Complete debonding of the fibre from the matrix has been predicted using the Griffith energy approach [6]. Further increase in the applied load eventually causes the fibre to be pulled out of the matrix. The energy required to pull out a tapered fibre is small because the energy transfer at the fibre–

matrix interface to overcome friction is small. In contrast, the energy required to pull out a uniform cylindrical fibre is large because the energy transfer at the fibre–matrix interface to overcome friction is large. The pull-out energies for the paraboloid and ellipsoid lay between those for the cylinder and the cone. These results may be intuitively obvious; we note that less energy is needed to puncture a material using a probe which features a tapered end than one with a blunt end and that the same argument holds when the probes are pulled out of the material. However, the results presented here allow this effect to be quantified. With the exception of the uniform cylindrical fibre which yields a constant energy density as demonstrated in Fig. 3, tapered fibres yield expressions for the energy density which depends on the fibre axial ratio,  $q$ , as defined in “Definitions”. Here, the energy density increases as  $q$  increases but plateaus out at large  $q$ . Defining the critical axial ratio,  $q_0$ , as the limit beyond which the energy density is independent of the fibre slenderness, our model predicts that  $q_0$  has a value of about 10 for tapered fibres.

Wisnom and Green [22] have predicted that if uniform cylindrical fibres, embedded in a matrix, are within a critical axial distance, these adjacent fibres could behave like a bundle and induce failure in shear in the vicinity of the bundle when the composite is subjected to high loads. Thereafter, the fibre bundle could be pulled out from the rest of the composite and, consequently, the composite suffers a catastrophic failure. We note that it remains to be seen if tapered fibres response in the same way to form bundles. In this case, how taper influences fibre interaction within the bundle and, consequently, the failure of the composite by fibre pull-out may be the subject for further investigation. It is anticipated that present studies in tissue engineering of nanofibre scaffolds, for achieving the appropriate bioactive and mechanical properties necessary to facilitate in vitro [23] and in vivo [24] cellular seeding and adhesion, will benefit from this knowledge. Here we note that reports have described the feasibility of growing tapered fibres from collagen materials in vitro in a cell-free enzyme/substrate, with varying surface area to volume ratio by controlling the enzyme to substrate ratio, by the process of self-assembly [25, 26]; this could be a step in the right direction towards the engineering of nanofibre

scaffolds. Experimental work on pullout of fibres, with different shapes, from a matrix would enable many of these conclusions to be tested. However, to the best of our knowledge no such experiments have yet been reported.

## References

1. Kim JK, Mai YW (1991) *Compos Sci Technol* 41:333
2. Lawrence P (1972) *J Mater Sci* 7:1. doi:10.1007/BF00549541
3. Piggott MR (1980) *Load bearing fibre composites*, 1st edn. Pergamon Press, Oxford
4. Kelly A, MacMillan NH (1986) *Strong solids: monographs on physics and chemistry of materials*, 3rd edn. Clarendon Press, Oxford
5. Suemasu H, Kondo A, Itatani K, Nozue A (2001) *Compos Sci Technol* 61:281
6. Bilteryst F, Marigo JJ (2003) *Eur J Mech A* 22:55
7. Quek MY (2002) *Int J Adhesion Adhesives* 22:303
8. Schuster DM, Scala E (1964) *Trans Metall Soc AIME* 230:1635
9. Carrara AS, McGarry FJ (1968) *J Compos Mater* 2:222
10. Goh KL, Aspden RM, Mathias KJ, Hukins DWL (1999) *Proc R Soc Lond A* 455:3351
11. Goh KL, Mathias KJ, Aspden RM, Hukins DWL (2000) *J Mater Sci* 35:2493. doi:10.1023/A:1004725903966
12. Goh KL, Aspden RM, Hukins DWL (2004) *Compos Sci Technol* 64:1091
13. Goh KL, Aspden RM, Mathias KJ, Hukins DWL (2004) *Proc R Soc Lond A* 460:2339
14. Goh KL, Huq AMA, Aspden RM, Hukins DWL (2008) *Adv Compos Lett* 17:131
15. Cox HL (1952) *Br J Appl Phys* 3:72
16. Gent AN, Chang YW, Nardin M, Schultz J (1996) *J Mater Sci* 31:1707. doi:10.1007/BF00372182
17. Goh KL, Meakin JR, Aspden RM, Hukins DWL (2005) *Proc R Soc Lond B* 272:1979
18. Goh KL, Meakin JR, Aspden RM, Hukins DWL (2007) *J Theor Biol* 245:305
19. Gent AN, Wang C (1993) *J Mater Sci* 28:2494. doi:10.1007/BF01151685
20. Chiang YC (2007) *J Mech* 23:95
21. Kelly A, Tyson WR (1965) *J Mech Phys Solids* 13:329
22. Wisnom MR, Green D (1995) *Composites* 26:499
23. Hosseinkhani H, Hosseinkhani M, Kobayashi H (2006) *J Bioactive Compat Polym* 21:277
24. Leo AJ, Grande DA (2006) *Cells Tissues Organs* 183:112
25. Holmes DF, Chapman JA, Prockop DJ, Kadler KE (1992) *Proc Natl Acad Sci USA* 89:9855
26. Holmes DF, Watson RB, Chapman JA, Kadler KE (1996) *J Mol Biol* 261:93